ANTIOXIDANTS & REDOX SIGNALING
Volume 9, Number 9, 2007

DOI: 10.1089/ars.2007.1665

# Forum Original Research Communication

# Lipid Raft–Mediated Uptake of Cysteine-Modified Thioredoxin-1: Apoptosis Enhancement by Inhibiting the Endogenous Thioredoxin-1

NORIHIKO KONDO,[1] YASUYUKI ISHII,[2] YONG-WON KWON,[1] MASAKI TANITO,[1] JUNKO SAKAKURA-NISHIYAMA,[1] MICHIKA MOCHIZUKI,[1] MICHIYUKI MAEDA,[1] SHIGO SUZUKI,[3,4] MASAMI KOJIMA,[3,4] YONG-CHUL KIM,[1] AOI SON,[1] HAJIME NAKAMURA,[5] and JUNJI YODOI[1,5]

## ABSTRACT

**Thioredoxin-1 (TRX) plays important roles in cellular signaling by controlling the redox state of cysteine residues in target proteins. TRX is released in response to oxidative stress and shows various biologic functions from the extracellular environment. However, the mechanism by which extracellular TRX transduces the signal into the cells remains unclear. Here we report that the cysteine modification at the active site of TRX promotes the internalization of TRX into the cells. TRX-C35S, in which the cysteine at residue 35 of the active site was replaced with serine, was internalized more effectively than wild-type TRX in human T-cell leukemia virus–transformed T cells. TRX-C35S bound rapidly to the cell surface and was internalized into the cells dependent on lipid rafts in the plasma membrane. This process was inhibited by wild-type TRX, reducing reagents such as dithiothreitol, and methyl-β-cyclodextrin, which disrupts lipid rafts. Moreover, the internalized TRX-C35S binds to endogenous TRX, resulting in the generation of intracellular reactive oxygen species (ROS) and enhanced *cis*-diamine-dichloroplatinum (II) (CDDP)-induced apoptosis *via* a ROS-mediated pathway involving apoptosis signal-regulating kinase-1 (ASK-1) activation. These findings suggest that the cysteine at the active site of TRX plays a key role in the internalization and signal transduction of extracellular TRX into the cells.** *Antioxid. Redox Signal.* 9, 1439–1448.

## INTRODUCTION

THIOREDOXIN-1 (TRX) is a ubiquitous 12-kDa protein with a redox-active disulfide within a conserved active site (-Cys-Gly-Pro-Cys-), which functions in concert with NADPH and TRX reductase (19, 35). Originally, human TRX was identified as adult T-cell leukemia (ATL)-derived factor (ADF) produced by the human T-cell leukemia virus type I (HTLV-I)-transformed T-cell line ATL2 (28). Several cytokine-like factors, including 3B6-IL-1 (34), eosinophil cytotoxicity-enhancing factor (ECEF) (2), the T-cell hybridoma MP6-derived B-cell growth factor (22), and early pregnancy factor (32), were identical or related to TRX, indicating that it plays multiple biologic roles both intracellularly and extracellularly (17, 18).

TRX is thought to reduce the oxidized form of target molecules in two steps: first, the reduced form of TRX [Trx-$(SH)_2$]

[1]Department of Biological Responses, Institute for Virus Research, Kyoto University, Kyoto, Japan.
[2]RIKEN Research Center for Allergy and Immunology, Clinical Allergy, Yokohama, Japan.
[3]Research Institute for Cell Engineering, National Institute of Advanced Industrial Science and Technology, Ikeda, Japan.
[4]Solution Oriented Research for Science and Technology (SORST) Japan Science and Technology Agency (JST), Kawaguchi, Japan.
[5]Thioredoxin Project, Translational Research Center Kyoto University Hospital, Kyoto, Japan.

binds to its target molecule *via* a nucleophilic attack by the thiolate of cysteine 32 (Cys32), forming a transient mixed disulfide bond with the target molecule; and second, a nucleophilic attack is carried out by the deprotonated Cys35, generating Trx-$S_2$ and a reduced form of the target molecule (9). Based on this theory, target molecules that bind directly to TRX have been identified by using a modified TRX in which Cys35 in the active site is replaced with serine (TRX-C35S). Many of the target molecules have been found to bind to a TRX-C35S column but not to a wild-type TRX column (1, 6, 16, 20, 33) (Fig. 1).

In the current study, we show that recombinant TRX-C35S (rTRX-C35S) binds to cells such as HTLV-I–transformed T cells (ATL2) or activated Jurkat T cells much more effectively than does recombinant wild-type TRX (rTRX-WT) and is internalized within 30 min in a process dependent on lipid rafts in the plasma membrane. Moreover, the internalized TRX-C35S then binds to endogenous TRX, resulting in the increased generation of intracellular reactive oxygen species (ROS) and enhanced *cis*-diamminedichloroplatinum (II) (CDDP)-induced apoptosis. The results presented here suggest that the cysteine at the active site of TRX plays a crucial role in the internalization and the signal transduction of extracellular TRX into the cells.

## MATERIALS AND METHODS

### *Cells, antibodies, and reagents*

The ATL2 and Jurkat T cells were cultured in RPMI 1640 medium containing 10% fetal calf serum (FCS) and antibiotics, as described previously (11). OptiPrep was purchased from Invitrogen Corp. (Carlsbad, CA). Other biochemical reagents were obtained from Nacalai Tesque (Kyoto, Japan). Anti-histidine (His) monoclonal antibody (mAb) was from Qiagen (Valencia, CA); mAbs against the transferrin receptor (Trf-R), Fyn, and caveolin-1 (Cav-1) were from Zymed Laboratories, Inc. (San Francisco, CA), anti-ASK-1 Ab (F-9) was from Santa Cruz Biotechnology, Inc. (Santa Cruz, CA), and anti-CD3 Ab (OKT3) was from eBioscience (San Diego, CA,).

### *Flow cytometry*

Cells were washed in Hank's balanced salt solution (HBSS) containing 0.1% FCS, and then incubated with rTRXs in HBSS. After washing with excess Cell Wash buffer (Becton Dickinson, La Jolla, CA), cells were analyzed by using a flow cytometer and Cell Quest software (Becton Dickinson).

### *Preparation of recombinant (r)TRXs and Alexa-labeled rTRXs*

Expression plasmids for His-tagged rTRX-WT, rTRX-CS (C32S/C35S) in which both Cys32 and Cys35 were replaced with serines, rTRX-C32S in which Cys32 was replaced with serine, and rTRX-C35S were prepared by polymerase chain reaction (PCR) for insertion into the *Bam*HI-*Sal*I site of the bacterial expression vector, pQE80L (Qiagen, U.K.) (11). These plasmids were introduced into competent *Escherichia coli* (XL-1 Blue) cells, and the transformants were cultured for 4 h [optical density at 650 nm ($OD_{650}$) = 0.6] in Terrific Broth (Invitrogen Corp.). The cells were harvested after incubation with 1 m*M* isopropyl-beta-D-thiogalactopyranoside (IPTG) for 2 h, and the rTRXs were purified with Ni-chelating magnetic beads (Promega, Madison, WI), according to the manufacturer's instructions. After PD-10 column chromatography, the purity of the rTRXs was verified by sodium dodecyl sulfate–polyacryl-

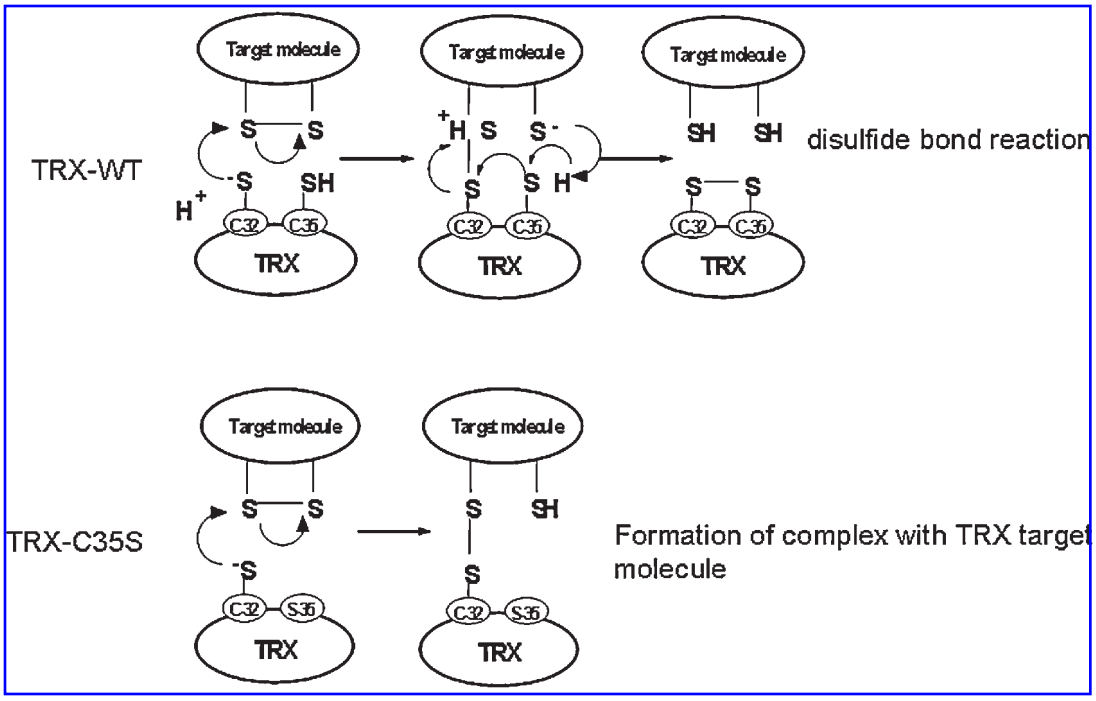


**FIG. 1. Mechanism of TRXs interaction with target molecules.**

amide gel electrophoresis (SDS-PAGE). The Alexa-labeled rTRXs were prepared by using an Alexa Fluor 488 protein-labeling kit (Invitrogen Corp.).

### *Confocal imaging*

Imaging was performed by using an RTS 2000 confocal laser microscope (Bio-Rad, Hercules, CA), which is a modified version of the Nikon RCM 8000video-rate confocal instrument.

### *Membrane labeling*

The surfaces of $2 \times 10^7$ ATL2 cells were labeled with a $4 \times 10^{-5}$ *M* PKH26 fluorescent stain kit (Zynaxis Inc., Malvern, PA). After incubation for 10 min at room temperature, the cells were washed with excess HBSS.

### *SDS-PAGE and Western blot analysis*

Samples were analyzed with 5–20% SDS-PAGE gradient gels (Ready Gels J; Bio-Rad) to analyze lipid rafts. The proteins separated by SDS-PAGE were transferred to polyvinylidene difluoride (PVDF) membranes (Millipore, Bedford, MA), which were incubated with appropriate primary Abs followed by secondary Abs conjugated to horseradish peroxidase. The bands were visualized with an ECL Western blot detection kit (GE Healthcare BioScience KK, Piscataway, NJ).

### *Preparation of membrane and cytosol fractions*

Cells were suspended in hypotonic buffer (50 m*M* HEPES (pH 7.6), 10 m*M* KCl, and 1 m*M* $MgCl_2$) containing protease inhibitors, and disrupted by nitrogen cavitation (800 psi). After centrifugation at 1,000 *g* for 10 min at 4°C, the supernatant was centrifuged at 50,000 rpm for 30 min to separate membrane and cytosolic fractions.

### *Gradient separation of rafts*

Rafts and nonraft fractions were separated by the method described in ref. 10, with slight modifications. All steps were carried out at 4°C. In brief, after treatment with 10 $\mu$g/ml rTRX-C35S for 1 h at 37°C, whole cells or membrane fractions were solubilized in 1% Triton X-100 in 10 m*M* Tris-HCl (pH 7.4), 150 m*M* NaCl, and 1 m*M* EDTA containing 10 $\mu$g/ml aprotinin, 1 m*M* PMSF, and 10 $\mu$g/ml leupeptin (STE buffer). The lysates were mixed with equal volumes of 60% OptiPrep solution. Samples (1 ml) were placed in ultracentrifuge tubes and overlaid with 8 ml of 25% OptiPrep, followed by 3.5 ml of 5% OptiPrep, both of which were diluted with STE buffer. The tubes were centrifuged at 40,000 rpm for 2 h. Fractions (1 ml) were collected from the top of the gradient. For SDS-PAGE and immunoblotting, two 1-ml fractions were combined and diluted with an equal volume of 2 × SDS sample buffer.

### *Cholesterol depletion*

Cells were treated with various concentrations of methyl-$\beta$-cyclodextrin (MCD) in HBSS containing 50 m*M* HEPES for 30 min at 37°C.

### *Stimulation of Jurkat T cells with Ab-coated beads*

Latex beads (6 $\mu$m) were coated with Abs as described previously (13, 29). Jurkat T cells were incubated with Ab-coated beads for 15 min at 37°C, and then with 100 ng/ml Alexa-labeled rTRX-C35S and Alexa (647)-labeled cholera toxin-B (CTx-B; Invitrogen Corp.) for 30 min. The cells were fixed for 10 min in 3.7% formaldehyde in phosphate-buffered saline (PBS).

### *Stimulation of Jurkat T cells with Ab-coated beads*

Latex beads (6 $\mu$m) were coated with Abs as described previously (13, 29). Jurkat T cells were incubated with Ab-coated beads for 15 min at 37°C, and then with 100 ng/ml Alexa-labeled rTRX-C35S and Alexa (647)-labeled cholera toxin-B (CTx-B; Invitrogen Corp.) for 30 min. The cells were fixed for 10 min in 3.7% formaldehyde in phosphate-buffered saline (PBS).

### *Measurement of intracellular reactive oxygen species*

Intracellular reactive oxygen species (ROS) were measured by using 2′,7′-dichlorofluorescein diacetate (DCFH-DA; Invitrogen Corp.) (30). This nonfluorescent membrane-diffusible dye is cleaved by intracellular esterases to release the acetyl group and produce nonfluorescent DCFH. Once trapped inside cells in the presence of ROS, this is modified to fluorescent DCFH, which can be excited with a 488-nm argon laser. Data were collected from at least 10,000 events and expressed as mean fluorescence intensities.

### *Detection of cell death with annexin V and PI*

Cell death was assessed by monitoring changes in cell size and granularity with flow cytometry, and by using annexin V-fluorescein isothiocyanate (FITC; Invitrogen Corp.) after exposure to phosphatidylserine (PS). Cell-membrane permeability was assessed by uptake of the DNA-binding fluorescent dye, propidium iodide (PI; Invitrogen Corp.) (14).

### *Immunoprecipitation*

Cells treated with rTRX-C35S were lysed with 1% Triton X-100 in buffer. The lysate was added to $Ni^+$-chelate beads or anti-ASK-1 Ab bound to protein A-sepharose (GE Healthcare Bio-Science KK) and rotated at 4°C.

## RESULTS

### *Binding and internalization of TRX-C35S in ATL2 cells*

ATL2 cells were incubated with 100 ng/ml Alexa (488)–labeled rTRX proteins (TRX-WT, TRX-CS, and TRX-C35S) for 30 min at 37°C, and the intensity of their fluorescence was de-

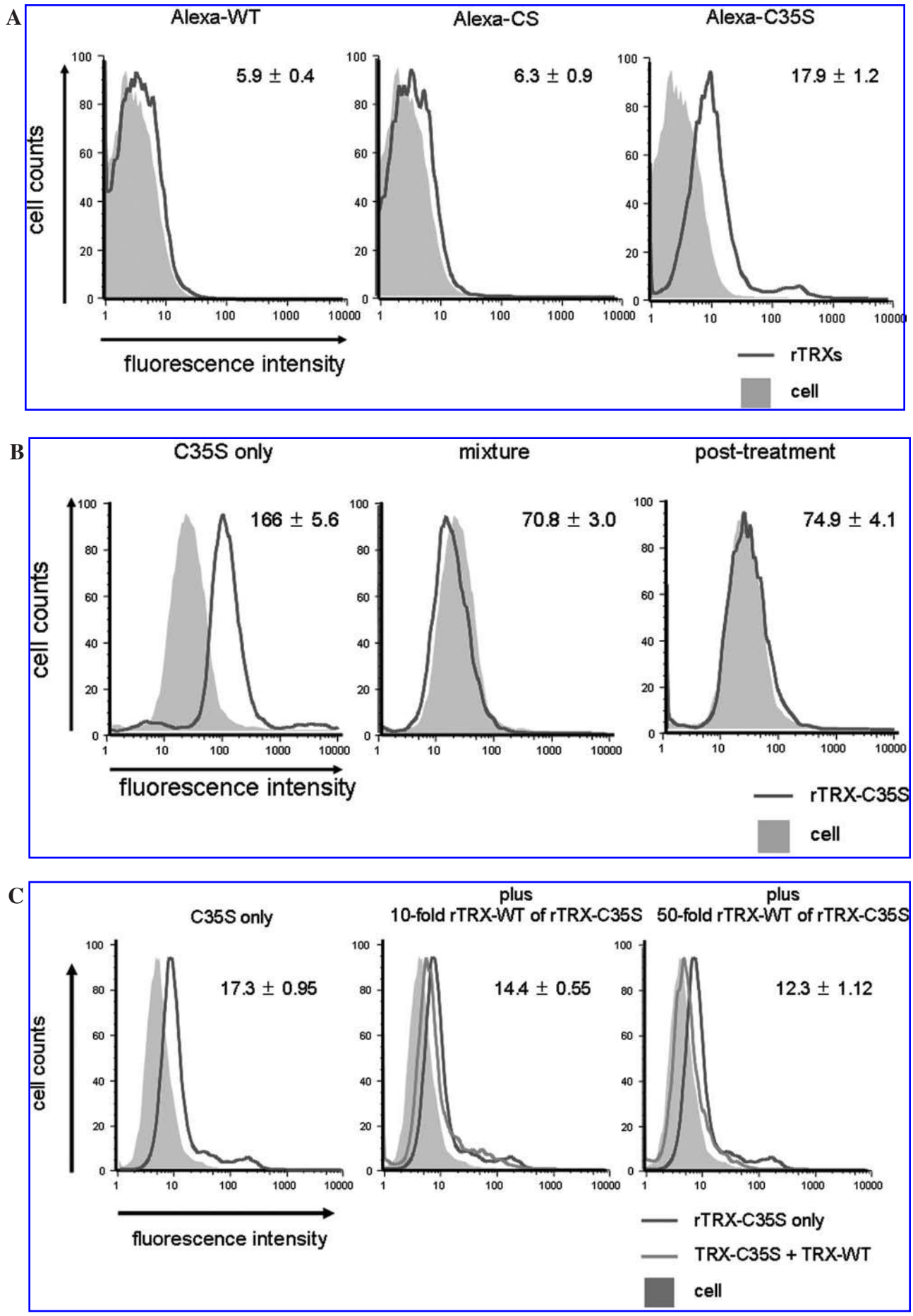
A
Alexa-WT
Alexa-CS
Alexa-C35S
5.9 ± 0.4
6.3 ± 0.9
17.9 ± 1.2
cell counts
fluorescence intensity
rTRXs
cell
B
C35S only
mixture
post-treatment
166 ± 5.6
70.8 ± 3.0
74.9 ± 4.1
cell counts
fluorescence intensity
rTRX-C35S
cell
C
C35S only
plus
10-fold rTRX-WT of rTRX-C35S
plus
50-fold rTRX-WT of rTRX-C35S
17.3 ± 0.95
14.4 ± 0.55
12.3 ± 1.12
cell counts
fluorescence intensity
rTRX-C35S only
TRX-C35S + TRX-WT
cell

tected by flow cytometry. As shown in Fig. 2A, the fluorescence peak of Alexa-labeled rTRX-C35S was markedly shifted right compared with that of rTRX-WT or rTRX-CS, indicating that Alexa-labeled rTRX-C35S bound rapidly to the cells, whereas Alexa-labeled rTRX-WT and Alexa-C32S/C35S did not.

Based on the biochemical theory (see Fig. 1), we investigated whether the binding of TRX-C35S was involved in the formation of disulfide bonds. ATL2 cells were treated with Alexa-labeled rTRX-C35S in the presence (Fig. 2B, mixture) or absence of 1 m*M* dithiothreitol (DTT). The treatment of the cells with 1 m*M* DTT for 30 min resulted in dissociation of the cell-bound TRX-C35S (Fig. 2B, after treatment). By contrast, the binding of Alexa-rTRX-C35S was not inhibited by the presence of an oxidizing reagent, such as 1 m*M* hydrogen peroxide ($H_2O_2$) (data not shown). Moreover, the binding of rTRX-C35S to the cells was also inhibited when the cells were incubated with 100 ng/ml Alexa-rTRX-C35S in the presence of a 10- or 50-fold excess of nonfluorescent rTRX-WT in a dose-dependent manner (Fig. 2C). These results indicate that formation of disulfide bonds is essential for the binding of rTRX-C35S to cell-surface target molecules, and TRX-WT and TRX-C35S may interact with the same target molecule on the cell surface.

To determine the distribution of TRX-C35S in ATL2 cells after the binding, ATL2 cells were incubated with 100 ng/ml Alexa-labeled rTRX-C35S for 30 min. Confocal microscopy showed green fluorescence with a heterogeneous dotlike distribution on the cell membrane (labeled with red fluorescence) in roughly 90% of cells (Fig. 3A, upper panels). In the remaining 10% of cells, the green fluorescence was homogeneously distributed (Fig. 3A, lower panels) in the experimental condition. No fluorescence was observed when cells were incubated with Alexa-labeled rTRX-WT or rTRX-CS (data not shown).

Western blot analysis confirmed that histidine (His)-tagged rTRX-C35S associated with both membrane and cytosolic fractions, whereas no binding of rTRX-WT and rTRX-CS was detected in either fraction (Fig. 3B).

When ATL2 cells were incubated with His-tagged rTRX-C35S in the presence of a 10-fold or 50-fold excess of rTRX-WT, the internalization of rTRX-C35S was inhibited by rTRX-WT in a dose-dependent manner (Fig. 3C). These results suggest that rTRX-WT competitively inhibited the internalization of rTRX-C35S by interacting with the same target molecule on the cell surface, because the binding and internalization of wild-type TRX *per se* to the cells is quite limited under the experimental conditions (Fig. 2A and D).

### *Involvement of lipid rafts in the internalization of TRX-C35S*

We further investigated whether rapid uptake of TRX-C35S might depend on the characteristics of the cell membrane. Because ATL-2 cells were reported to have lipid rafts on the cell membranes (8), we focused on the formation of lipid-raft microdomains. Raft fractions were prepared from ATL2 cells by flotation through OptiPrep gradients, and their purity was confirmed by measuring their cholesterol content and detecting the raft marker protein, Cav-1. ATL2 cells incubated with 10 $\mu$g/ml His-tagged rTRX-C35S for 1 h were lysed, and then fractionated. Western blot analysis showed that rTRX-C35S was present in several fractions, including fraction 2, in which Cav-1 was detected (Fig. 4A). This suggested that a portion of rTRX-C35S was associated with lipid-raft microdomains. However, a large proportion of the rTRX-C35S was recovered in the high-density nonraft fraction (fraction 6). It seemed likely that the rTRX-C35S had already entered the cytosol (Fig. 3A and B); thus, we repeated the raft fractionation with the membrane fraction of cells incubated with 10 $\mu$g/ml His-tagged rTRX-C35S. The results clearly showed that rTRX-C35S was associated almost exclusively with rafts in the membrane fraction (Fig. 4B). Moreover, methyl-$\beta$-cyclodextrin (MCD), which disrupts lipid rafts, inhibited the binding and internalization of rTRX-C35S in a dose-dependent manner (Fig. 4C). At these concentrations, MCD did not cause cell death, as determined by trypan blue staining. These results suggest that internalization of rTRX-C35S into ATL2 cells was dependent on lipid-rafts structure.

The internalization of rTRX-C35S changes the intracellular redox state through the inhibition of endogenous TRX activity and cellular sensitivity to apoptosis. To clarify the meaning of the internalization of cysteine-modified TRX into the cells, we investigated the intracellular redox state by measuring the generation of intracellular ROS. Further to explore the biologic effects of internalized rTRX-C35S, we used Jurkat T cells undergoing stress-induced apoptosis triggered by anticancer agent *cis*-diamminedichloroplatinum (CDDP). Jurkat T cells were incubated with 10 $\mu$g/ml rTRX-C35S for 1 h before treatment with 30 $\mu$g/ml CDDP, and the rate of ROS production was measured (Fig. 5A). ROS production in cells treated with CDDP alone began to increase at 2 h and reached a maximum at 6 h; ROS levels were substantially increased in cells treated with 10 $\mu$g/ml rTRX-C35S for 1 h before exposure to CDDP.

We next examined the possible interaction between internalized rTRX-C35S and endogenous TRX. Jurkat transfectants stably expressing FLAG-tagged TRX-WT were treated with 10

**FIG. 2. Binding of TRX-C35S to ATL2 cells.** (**A**) Flow-cytometry analysis for the binding of TRX molecules to ATL2 cells. The cells were incubated with 100 ng/ml Alexa-labeled rTRX-WT (left), rTRX-CS (*center*), or rTRX-C35S (right). Cells treated with rTRXs (*black line*), and untreated cells (*grey*) are shown. Data are expressed as MFI mean ± standard deviation (SD; $n = 3$). (**B**) Flow cytometry analysis for disulfide bond–dependent binding of rTRX-C35S in ATL2 cells. Cells were incubated with Alexa-labeled rTRX-C35S alone, or in the presence of 1 m*M* DTT. A portion of the rTRX-C35S–treated cells was treated with 1 m*M* DTT (after treatment). Fluorescence of bound Alexa-labeled rTRX-C35S (*black line*) and untreated cells (*grey*) also is shown. Data are expressed as MFI mean ± standard deviation (SD; $n = 3$). (**C**) Flow-cytometry analyses of inhibition of TRX-C35S binding by rTRX-WT. ATL2 cells were incubated with 100 ng/ml rTRX-C35S in the presence or absence of 10 or 50 $\mu$g/ml nonfluorescent rTRX-WT. The treated ATL2 cells with Alexa-labeled rTRX-C35S alone (*black line*), Alexa-labeled rTRX-C35S in the presence of 10 or 50 $\mu$g/ml of nonfluorescent rTRX-WT (*dark grey line*), or untreated cells (*grey*) are shown. Data are expressed as MIF mean ± standard deviation (SD; $n = 3$).

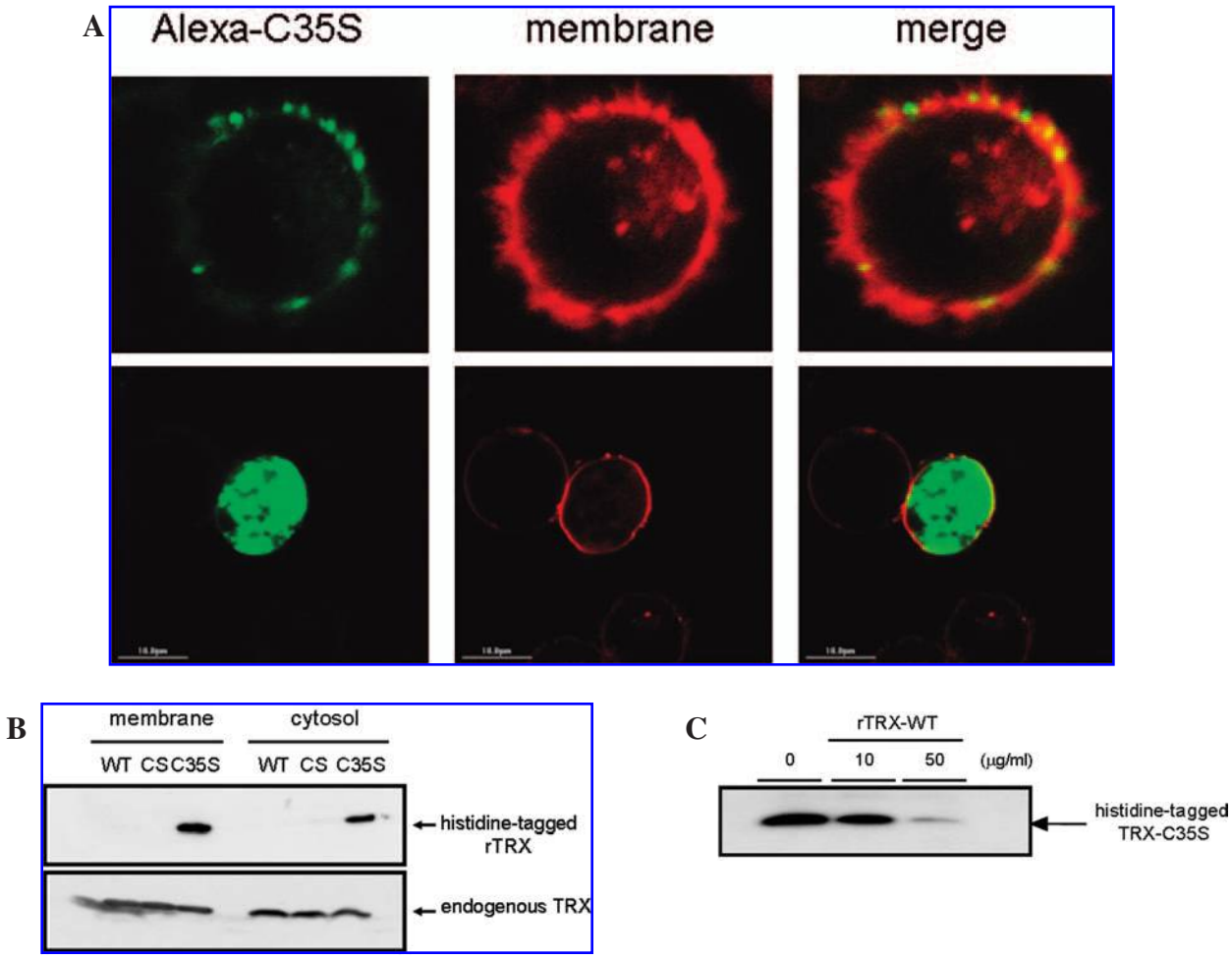


**FIG. 3. Internalization of TRX-C35S by ATL2 cells.** **A**, Confocal analysis of internalization of rTRX-C35S in ATL2 cells. Cells were incubated with 100 ng/ml Alexa-labeled rTRX-C35S for 30 min, and their membranes were stained with PKH26. *Left:* Alexa-rTRX-C35S-labeled image. Middle: PKH26-labeled image. Right: left and middle images superimposed. *Upper panels:* in the majority of cells, Alexa labeling was located in the plasma membrane. *Lower panels:* In 10% of the cells, Alexa labeling was located mainly in the cytosol. (**B**) Western blots of exogenous TRX molecules internalized by ATL2 cells incubated with 10 $\mu$g/ml His-tagged rTRX-WT (WT), rTRX-C32S/C35S (CS), or rTRX-C35S (C35S) for 1 h. The ligands were identified with anti-His mAb (*upper panel*) and anti-TRX mAb (*lower panel*). (**C**) Western blot analysis of inhibition of TRX-C35S internalization by rTRX-WT. ATL2 cells were incubated with 1 $\mu$g/ml His-tagged rTRX-C35S in the presence or absence of 10 or 50 $\mu$g/ml rTRX-WT. TRX-C35S was detected in the cytosol fraction with anti-His mAb (*lower panel*).

$\mu$g/ml rTRX-C35S for 1 h and then incubated with or without 3 $\mu$g/ml CDDP. As shown in Fig. 5B, internalization of rTRX-C35S was markedly increased by CDDP, and complex formation between endogenous TRX and rTRX-C35S also was enhanced. This suggests that rTRX-C35S facilitates CDDP-induced apoptosis partly by inhibiting the antiapoptotic activity of endogenous TRX. As TRX binds to ASK-1 *via* disulfide bonds and inhibits this stress kinase pathway (24), we tested whether the CDDP-induced dissociation of TRX from ASK-1 was enhanced by rTRX-C35S. Jurkat T cells pretreated with 10 $\mu$g/ml rTRX-C35S for 1 h were cultured in the presence or absence of 30 $\mu$g/ml CDDP for 3 h. As shown in Fig. 5C, the dissociation of TRX from ASK-1 in cells treated with rTRX-C35S and CDDP was markedly greater than that in cells treated with CDDP alone. Together, these results suggest that internalized rTRX-C35S facilitates CDDP-induced apoptosis by inhibiting endogenous TRX activity and enhancing the ROS-mediated or ASK-1–dependent apoptotic pathways or both.

The progression of apoptosis was determined by both annexin V-FITC staining and PI uptake (14). When Jurkat cells were exposed to 3 $\mu$g/ml CDDP, 32% were found to be in the early phase of apoptosis (annexin V positive–PI negative) and 7.7% were in the late phase of apoptosis (annexin V positive–PI positive) (Fig. 5D). The proportions of cells in the early and late phases of apoptosis were increased to 45% and 20%, respectively, by incubation with 10 $\mu$g/ml rTRX-C35S for 1 h before CDDP exposure. Late-phase apoptosis was further increased to 29% by 3 h preincubation with rTRX-C35S.

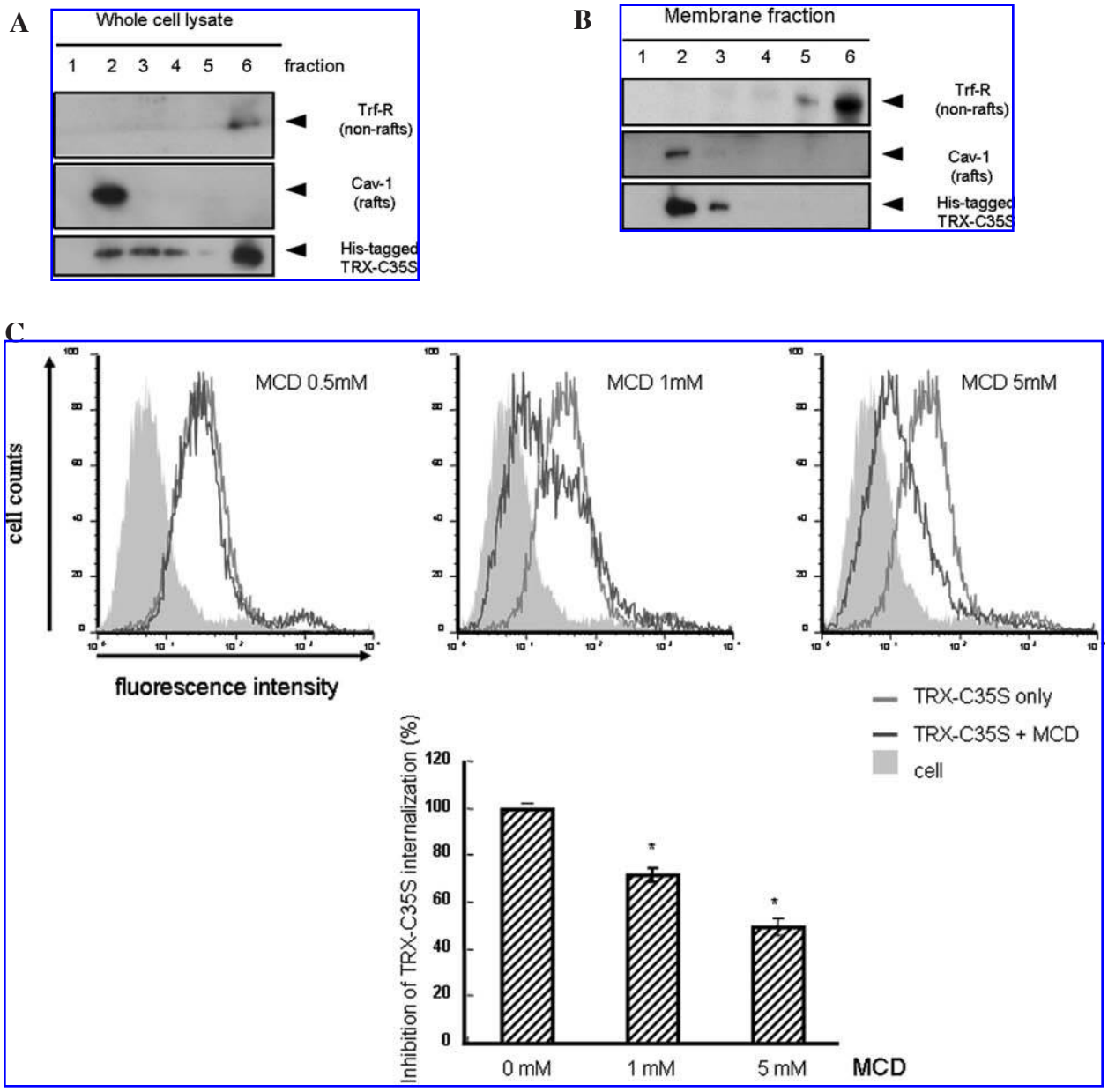


**FIG. 4. Localization of rTRX-C35S in lipid-raft microdomains.** (**A**) Western blot analysis of rTRX-C35S in raft fractions from whole-cell lysates of ATL2 cells. ATL2 cells were incubated with 10 $\mu$g/ml rTRX-C35S for 1 h, and raft fractions were prepared from whole-cell lysates. The distributions of Trf-R, Cav-1, and rTRX-C35S were visualized by using appropriate Abs. (**B**) Western blot analysis of rTRX-C35S in raft fractions prepared from ATL2 cell membranes. ATL2 cells were incubated with 10 $\mu$g/ml rTRX-C35S for 1 h, and raft fractions were prepared from the membrane fraction of ATL2 cells. (**C**) Effect of TRX-C35S internalization on the disruption of lipid-raft structures. ATL2 cells, treated in the presence or absence of MCD, were incubated with 100 ng/ml Alexa-labeled rTRX-C35S for 30 min, and their fluorescence intensity was analyzed with flow cytometry. Data are expressed as mean $\pm$ standard deviation (SD; $n = 3$). The $p$ values were calculated by one-way analysis of variance (ANOVA) followed by Sheffé tests. *$p < 0.01$ *versus* MCD, 0 m*M*).

## DISCUSSION

In the present study, we showed that rTRX-C35S was rapidly internalized into HTLV-I–transformed T cells as well as CDDP-treated Jurkat T cells. Recombinant (r)TRX-C35S bound to ATL2 cells much more effectively than did wild-type rTRX and provided evidence that a disulfide bond is involved in the binding of rTRX-C35S onto the cell surface (Fig. 2A and B). We also prepared another recombinant mutant TRX, such as rTRX-CS or rTRX-C32S, and analyzed its binding to the cells. However, both rTRX-CS and rTRX-C32S failed to bind to ATL2 cells (Fig. 2A; data not shown). These results collectively in-

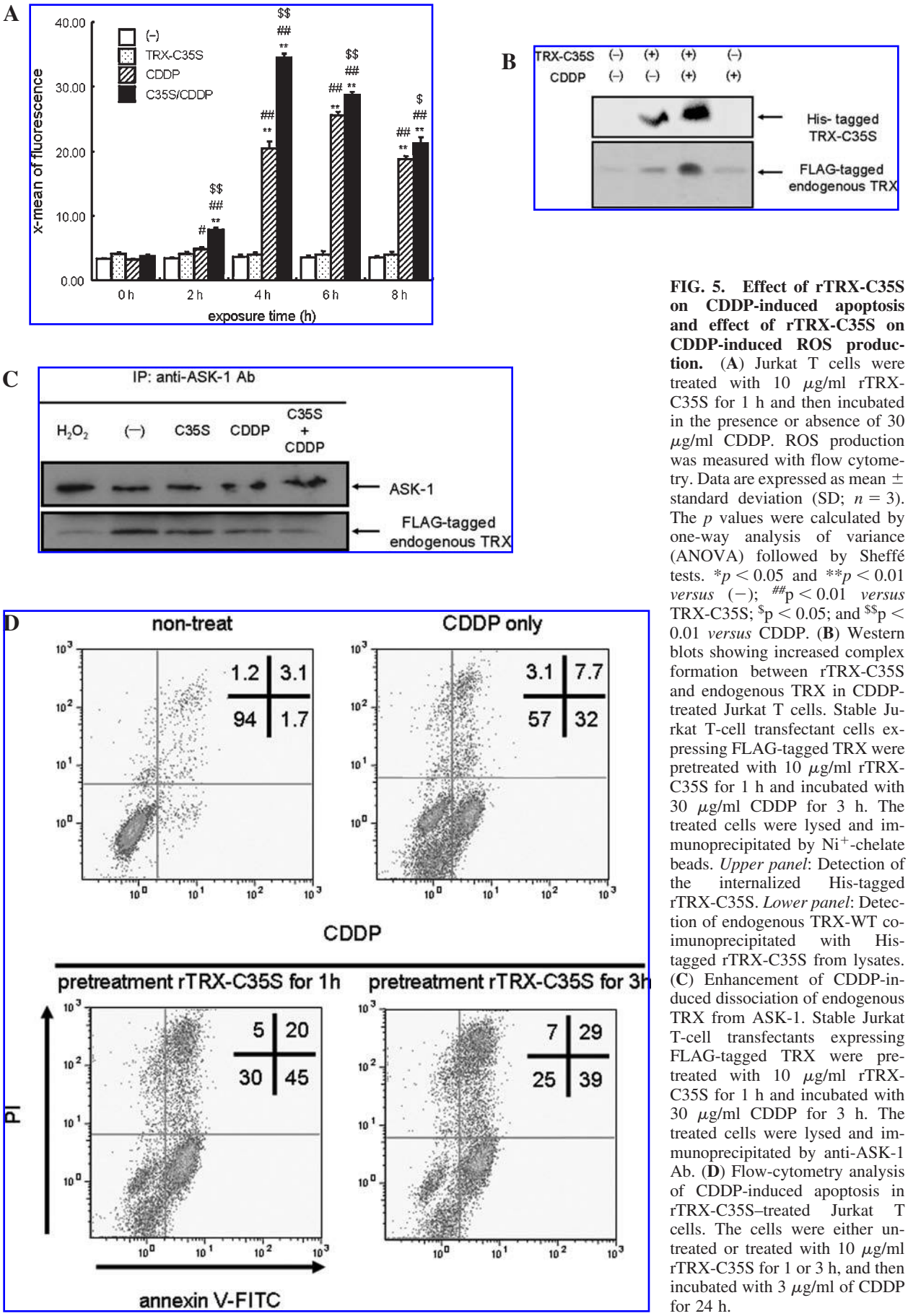


**FIG. 5. Effect of rTRX-C35S on CDDP-induced apoptosis and effect of rTRX-C35S on CDDP-induced ROS production.** (**A**) Jurkat T cells were treated with 10 $\mu$g/ml rTRX-C35S for 1 h and then incubated in the presence or absence of 30 $\mu$g/ml CDDP. ROS production was measured with flow cytometry. Data are expressed as mean $\pm$ standard deviation (SD; $n = 3$). The $p$ values were calculated by one-way analysis of variance (ANOVA) followed by Sheffé tests. $^{*}p < 0.05$ and $^{**}p < 0.01$ *versus* (−); $^{\#\#}p < 0.01$ *versus* TRX-C35S; $^{\$}p < 0.05$; and $^{\$\$}p < 0.01$ *versus* CDDP. (**B**) Western blots showing increased complex formation between rTRX-C35S and endogenous TRX in CDDP-treated Jurkat T cells. Stable Jurkat T-cell transfectant cells expressing FLAG-tagged TRX were pretreated with 10 $\mu$g/ml rTRX-C35S for 1 h and incubated with 30 $\mu$g/ml CDDP for 3 h. The treated cells were lysed and immunoprecipitated by $Ni^{+}$-chelate beads. *Upper panel*: Detection of the internalized His-tagged rTRX-C35S. *Lower panel*: Detection of endogenous TRX-WT coimunoprecipitated with His-tagged rTRX-C35S from lysates. (**C**) Enhancement of CDDP-induced dissociation of endogenous TRX from ASK-1. Stable Jurkat T-cell transfectants expressing FLAG-tagged TRX were pretreated with 10 $\mu$g/ml rTRX-C35S for 1 h and incubated with 30 $\mu$g/ml CDDP for 3 h. The treated cells were lysed and immunoprecipitated by anti-ASK-1 Ab. (**D**) Flow-cytometry analysis of CDDP-induced apoptosis in rTRX-C35S–treated Jurkat T cells. The cells were either untreated or treated with 10 $\mu$g/ml rTRX-C35S for 1 or 3 h, and then incubated with 3 $\mu$g/ml of CDDP for 24 h.

dicate that Cys32, but not Cys35, Cys62, Cys69, and Cys73, in TRX is indispensable for its binding to the target molecules on the cell surface.

The present experiments provide evidence that rTRX-C35S is localized to lipid rafts, which are conserved and critical structures for signal transduction from cell-surface receptors (5, 26). Not only membrane signaling, but also exocytosis, endocytosis, and virus entry are associated with lipid-raft structures (4, 21). Cav-1 is a major protein and was the first molecular marker of caveolae (a type of raft microdomain) to be identified (12, 23). Hatanaka *et al.* (8) reported that Cav-1 was expressed in HTLV-I–transformed T cells. Reports suggest that lipid rafts are induced by various stimuli, including viral transformation, which supports the idea that the enhanced internalization of rTRX-C35S in HTLV-I–transformed ATL2 cells is closely correlated with lipid-raft formation (Fig. 4A–C). We confirmed the occurrence of higher levels of internalization of rTRX-C35S in several HTLV-I–transformed T-cell lines compared with HTLV-I–negative cell lines (data not shown). Moreover, we found that exogenous rTRX-C35S was not taken up by nonactivated T cells, but rather accumulated in raft structures in Jurkat T cells stimulated with anti-CD3–coated beads or with PMA and ionomycin. Raft fractionation and confocal analysis also showed that the level of rTRX-C35S increased in the activated Jurkat T cells (Hara *et al*., unpublished data). These results suggest that internalization of rTRX-C35S is dependent on the formation of lipid-raft microdomains in the plasma membrane in activated and virus-transformed T cells.

Many molecules on the membranes of T cells are candidates for TRX-binding molecules because they associate with signaling or adaptor molecules with conserved cysteine residues and have an affinity for lipid rafts. One such candidate molecule is CD4, which forms complexes in rafts and is the major receptor for human immunodeficiency virus (HIV) entry. The immunoglobulin-like domain, D2, in CD4 is redox sensitive and is reportedly regulated by TRX (15). However, it is unlikely that CD4 is the major TRX target molecule, as the level of CD4 expression is not changed by activation of Jurkat T cells. Alternatively, endogenous TRX itself, which is induced in the plasma membrane of activated T cells, might be the target molecule responsible for the internalization of rTRX-C35S. We also observed that rTRX-C35S binds on the cell surface of human umbilical vein endothelial cells as well as T cells (Hara T *et al*., unpublished data). Moreover, we found that rTRX-C35S interacted with endogenous TRX (Fig. 5B). Moreover, we observed that endogenous TRX *per se* bound to the TRX-family proinflammatory molecule, MIF (macrophage migration inhibitory factor), and inhibited MIF entry into the cells (Kato *et al*., unpublished data). We are now investigating other TRX target molecules in lipid rafts by using TRX-C35S affinity columns and two-dimensional electrophoresis.

The biological significance of the internalization of TRX-C35S was observed in the change of intracellular redox state and the sensitivity to the anticancer agent CDDP. The present results showed that the internalization of TRX-C35S enhanced the CDDP-induced generation of intracellular ROS and cellular apoptosis (Fig. 5A and D). Direct interaction of rTRX-C35S with endogenous TRX might also result in the dissociation of TRX from ASK-1, leading to activation of an ASK-1–mediated apoptotic signal cascade (Fig. 5B and C). These results shed light on the mechanisms by which extracellular TRX transduces the signals into the cells.

We consider that the posttranslational modification of endogenous TRX on Cys35 might enable it to enter cells in a lipid raft–mediated pathway similar to rTRX-C35S. Indeed, increasing evidence suggests that active site or other cysteine residues of TRX or both can be posttranslationally modified by *N*-nitrosylation, glutathionylation, or cysteinylation, and impart different activities to native TRX (3, 7, 25, 27, 31). Therefore, we speculate that cysteine 35 of TRX might be modified *via* disulfide bond, causing the internalization of TRX from the extracellular environment. We are also exploring the cysteine-modified TRX in the supernatant of virus-transformed T cells as well as the activated T cells.

In conclusion, our data show that rTRX-C35S can be internalized through lipid rafts on the plasma membrane of activated T cells, thereby affecting the intracellular redox balance. The rapid uptake of rTRX-C35S *via* lipid rafts might represent a fundamental mechanism of cross-talk that is particularly important for modulating the oxidative stress responses.

## ACKNOWLEDGMENTS

We thank Dr. K. Ishizaka for help with preparation of the manuscript; Dr. A. Nishiyama and Dr. H. Masutani for the discussion and technical support; Dr. J. Bai, Y Yamaguchi, A. Teratani, and R. Otsuki for help with technical assistance; and C. Kubo and M. Hasegawa for secretarial help. This study was supported by a grant-in-Aid for Scientific Research from the Ministry of Education, Culture, Sports, Science and Technology of Japan, and by a Grant-in-Aid from the Research and Development Program for New Bio-Industry Initiatives.

## ABBREVIATIONS

ATL, adult T-cell leukemia; Cav, caveolin; CDDP, *cis*-diamine-dichloroplatinum (II); CS, C32S/C35S; His, histidine; HTLV-I, human T-cell leukemia virus type I; MCD, methyl-$\beta$-cyclodextrin; PMA, phorbol 12-myristate 13-acetate; ROS, reactive oxygen species; TRX, thioredoxin-1;Trf-R, transferrin receptor; WT, wild-type.

## REFERENCES

1. Anelli T, Alessio M, Mezghrani A, Simmen T, Talamo F, Bachi A, and Sitia R. ERp44, a novel endoplasmic reticulum folding assistant of the thioredoxin family. *EMBO J* 21: 835–844, 2002.
2. Balcewicz-Sablinska MK, Wollman EE, Gorti R, and Silberstein DS. Human eosinophil cytotoxicity-enhancing factor, II: Multiple forms synthesized by U937 cells and their relationship to thioredoxin/adult T cell leukemia-derived factor. *J Immunol* 147: 2170–2174, 1991.
3. Casagrande S, Bonetto V, Fratelli M, Gianazza E, Eberini I, Massignan T, Salmona M, Chang G, Holmgren A, and Ghezzi P. Glutathionylation of human thioredoxin: a possible crosstalk between the glutathione and thioredoxin systems. *Proc Natl Acad Sci U S A* 99: 9745–9749, 2002.

4. Chazal N and Gerlier D. Virus entry, assembly, budding, and membrane rafts. *Microbiol Mol Biol Rev* 67: 226–237, table of contents, 2003.
5. Dykstra M, Cherukuri A, Sohn HW, Tzeng SJ, and Pierce SK. Location is everything: lipid rafts and immune cell signaling. *Annu Rev Immunol* 21: 457–481, 2003.
6. Fomenko DE and Gladyshev VN. CxxS: fold-independent redox motif revealed by genome-wide searches for thiol/disulfide oxidoreductase function. *Protein Sci* 11: 2285–2296, 2002.
7. Haendeler J, Hoffmann J, Tischler V, Berk BC, Zeiher AM, and Dimmeler S. Redox regulatory and anti-apoptotic functions of thioredoxin depend on S-nitrosylation at cysteine 69. *Nat Cell Biol* 4: 743–749, 2002.
8. Hatanaka M, Maeda T, Ikemoto T, Mori H, Seya T, and Shimizu A. Expression of caveolin-1 in human T cell leukemia cell lines. *Biochem Biophys Res Commun* 253: 382–387, 1998.
9. Holmgren A. Thioredoxin structure and mechanism: conformational changes on oxidation of the active-site sulfhydryls to a disulfide. *Structure* 3: 239–243, 1995.
10 Kawabuchi M, Satomi Y, Takao T, Shimonishi Y, Nada S, Nagai K, Tarakhovsky A, and Okada M. Transmembrane phosphoprotein Cbp regulates the activities of Src-family tyrosine kinases. *Nature* 404: 999–1003, 2000.
11. Kondo N, Ishii Y, Kwon YW, Tanito M, Horita H, Nishinaka Y, Nakamura H, and Yodoi J. Redox-sensing release of human thioredoxin from T lymphocytes with negative feedback loops. *J Immunol* 172: 442–448, 2004.
12. Kurzchalia TV, Dupree P, Parton RG, Kellner R, Virta H, Lehnert M, and Simons K. VIP21, a 21-kD membrane protein is an integral component of trans-Golgi-network-derived transport vesicles. *J Cell Biol* 118: 1003–1014, 1992.
13. Lowin-Kropf B, Shapiro VS, and Weiss A. Cytoskeletal polarization of T cells is regulated by an immunoreceptor tyrosine-based activation motif-dependent mechanism. *J Cell Biol* 140: 861–871, 1998.
14. Martin SJ, Reutelingsperger CP, McGahon AJ, Rader JA, van Schie RC, LaFace DM, and Green DR. Early redistribution of plasma membrane phosphatidylserine is a general feature of apoptosis regardless of the initiating stimulus: inhibition by overexpression of Bcl-2 and Abl. *J Exp Med* 182: 1545–1556, 1995.
15. Matthias LJ, Yam PT, Jiang XM, Vandegraaff N, Li P, Poumbourios P, Donoghue N, and Hogg PJ. Disulfide exchange in domain 2 of CD4 is required for entry of HIV-1. *Nat Immunol* 3: 727–732, 2002.
16. Motohashi K, Kondoh A, Stumpp MT, and Hisabori T. Comprehensive survey of proteins targeted by chloroplast thioredoxin. *Proc Natl Acad Sci U S A* 98: 11224–11229, 2001.
17. Nakamura H, De Rosa SC, Yodoi J, Holmgren A, Ghezzi P, and Herzenberg LA. Chronic elevation of plasma thioredoxin: inhibition of chemotaxis and curtailment of life expectancy in AIDS. *Proc Natl Acad Sci U S A* 98: 2688–2693, 2001.
18. Nakamura H, Herzenberg LA, Bai J, Araya S, Kondo N, Nishinaka Y, and Yodoi J. Circulating thioredoxin suppresses lipopolysaccharide-induced neutrophil chemotaxis. *Proc Natl Acad Sci U S A* 98: 15143–15148, 2001.
19. Nakamura H, Nakamura K, and Yodoi J. Redox regulation of cellular activation. *Annu Rev Immunol* 15: 351–369, 1997.
20. Norgaard P and Winther JR. Mutation of yeast Eug1p CXXS active sites to CXXC results in a dramatic increase in protein disulphide isomerase activity. *Biochem J* 358: 269–274, 2001.
21. Parton RG and Richards AA. Lipid rafts and caveolae as portals for endocytosis: new insights and common mechanisms. *Traffic* 4: 724–738, 2003.
22. Rosen A, Lundman P, Carlsson M, Bhavani K, Srinivasa BR, Kjellstrom G, Nilsson K, and Holmgren A. A CD4+ T cell line-secreted factor, growth promoting for normal and leukemic B cells, identified as thioredoxin. *Int Immunol* 7: 625–633, 1995.
23. Rothberg KG, Heuser JE, Donzell WC, Ying YS, Glenney JR, and Anderson RG. Caveolin, a protein component of caveolae membrane coats. *Cell* 68: 673–682, 1992.
24. Saitoh M, Nishitoh H, Fujii M, Takeda K, Tobiume K, Sawada Y, Kawabata M, Miyazono K, and Ichijo H. Mammalian thioredoxin is a direct inhibitor of apoptosis signal-regulating kinase (ASK) 1. *EMBO J* 17: 2596–2606, 1998.
25. Shibata T, Yamada T, Ishii T, Kumazawa S, Nakamura H, Masutani H, Yodoi J, and Uchida K. Thioredoxin as a molecular target of cyclopentenone prostaglandins. *J Biol Chem* 278: 26046–26054, 2003.
26. Simons K and Toomre D. Lipid rafts and signal transduction. *Nat Rev Mol Cell Biol* 1: 31–39, 2000.
27. Sumbayev VV. *S*-Nitrosylation of thioredoxin mediates activation of apoptosis signal-regulating kinase 1. *Arch Biochem Biophys* 415: 133–136, 2003.
28. Tagaya Y, Maeda Y, Mitsui A, Kondo N, Matsui H, Hamuro J, Brown N, Arai K, Yokota T, Wakasugi H, and Yodoi J. ATL-derived factor (ADF), an IL-2 receptor/Tac inducer homologous to thioredoxin: possible involvement of dithiol-reduction in the IL-2 receptor induction. *EMBO J* 8: 757–764, 1989.
29. Tanimura N, Nagafuku M, Minaki Y, Umeda Y, Hayashi F, Sakakura J, Kato A, Liddicoat DR, Ogata M, Hamaoka T, and Kosugi A. Dynamic changes in the mobility of LAT in aggregated lipid rafts upon T cell activation. *J Cell Biol* 160: 125–135, 2003.
30. Tanito M, Kwon YW, Kondo N, Bai J, Masutani H, Nakamura H, Fujii J, Ohira A, and Yodoi J. Cytoprotective effects of geranylgeranylacetone against retinal photooxidative damage. *J Neurosci* 25: 2396–2404, 2005.
31. Tao L, Gao E, Bryan NS, Qu Y, Liu HR, Hu A, Christopher TA, Lopez BL, Yodoi J, Koch WJ, Feelisch M, and Ma XL. Cardioprotective effects of thioredoxin in myocardial ischemia and reperfusion: role of S-nitrosation [corrected]. *Proc Natl Acad Sci U S A* 101: 11471–11476, 2004.
32. Tonissen KF and Wells JR. Isolation and characterization of human thioredoxin-encoding genes. *Gene* 102: 221–228, 1991.
33. Verdoucq L, Vignols F, Jacquot JP, Chartier Y, and Meyer Y. In vivo characterization of a thioredoxin h target protein defines a new peroxiredoxin family. *J Biol Chem* 274: 19714–19722, 1999.
34. Wakasugi N, Tagaya Y, Wakasugi H, Mitsui A, Maeda M, Yodoi J, and Tursz T. Adult T-cell leukemia-derived factor/thioredoxin, produced by both human T-lymphotropic virus type I- and Epstein-Barr virus-transformed lymphocytes, acts as an autocrine growth factor and synergizes with interleukin 1 and interleukin 2. *Proc Natl Acad Sci U S A* 87: 8282–8286, 1990.
35. Yodoi J and Uchiyama T. Diseases associated with HTLV-I: virus, IL-2 receptor dysregulation and redox regulation. *Immunol Today* 13: 405–411, 1992.

Address reprint requests to:
*Norihiko Kondo, Ph.D.*
*Junji Yodoi, M.D. Ph.D.*
*Department of Biological Responses*
*Institute for Virus Research*
*Kyoto University*
*53, Kawahara-cho, Shogoin*
*Sakyo, Kyoto 606-8607, Japan*

*E-mail:* nkondoh-ivr@umin.ac.jp
yodoi@virus.kyoto-u.ac.jp

Date of first submission to ARS Central, March 28, 2007; date of final revised submission, March 28, 2007; date of acceptance, March 29, 2007.

**This article has been cited by:**


1. Atsushi Nakajima, Toshiro Fukui, Yu Takahashi, Masanobu Kishimoto, Masao Yamashina, Shinji Nakayama, Yutaku Sakaguchi, Katsunori Yoshida, Kazushige Uchida, Akiyoshi Nishio, Junji Yodoi, Kazuichi Okazaki. 2012. Attenuation of indomethacin-induced gastric mucosal injury by prophylactic administration of sake yeast-derived thioredoxin. *Journal of Gastroenterology* **47**:9, 978-987. [CrossRef]
2. Si Jin , Fan Zhou , Foad Katirai , Pin-Lan Li . Lipid Raft Redox Signaling: Molecular Mechanisms in Health and Disease. *Antioxidants & Redox Signaling*, ahead of print. [Abstract] [Full Text HTML] [Full Text PDF] [Full Text PDF with Links]
3. Shouji Matsushima, Daniela Zablocki, Junichi Sadoshima. 2010. Application of recombinant thioredoxin1 for treatment of heart disease. *Journal of Molecular and Cellular Cardiology* . [CrossRef]
4. Xing-Tao CHEN, Gui-Tang WANG. 2010. ANALYSIS OF UP-REGULATED GENES IN CAENORHABDITIS ELEGANS TREATED WITH FORMALIN. *Acta Hydrobiologica Sinica* **34**:1, 35-42. [CrossRef]
5. Md. Kaimul Ahsan , Hajime Nakamura , Junji Yodoi Redox Regulation by Thioredoxin in Cardiovascular Diseases 159-165. [Abstract] [Summary] [Full Text PDF] [Full Text PDF with Links]
6. Md. Kaimul Ahsan , Istvan Lekli , Diptarka Ray , Junji Yodoi , Dipak K. Das . 2009. Redox Regulation of Cell Survival by the Thioredoxin Superfamily: An Implication of Redox Gene Therapy in the Heart. *Antioxidants & Redox Signaling* **11**:11, 2741-2758. [Abstract] [Full Text HTML] [Full Text PDF] [Full Text PDF with Links]
7. Aoi Son , Noriko Kato , Tomohisa Horibe , Yoshiyuki Matsuo , Michika Mochizuki , Akira Mitsui , Koji Kawakami , Hajime Nakamura , Junji Yodoi . 2009. Direct Association of Thioredoxin-1 (TRX) with Macrophage Migration Inhibitory Factor (MIF): Regulatory Role of TRX on MIF Internalization and Signaling. *Antioxidants & Redox Signaling* **11**:10, 2595-2605. [Abstract] [Full Text HTML] [Full Text PDF] [Full Text PDF with Links] [Supplemental material]
8. Hajime Nakamura, Yuma Hoshino, Hiroaki Okuyama, Yoshiyuki Matsuo, Junji Yodoi. 2009. Thioredoxin 1 delivery as new therapeutics. *Advanced Drug Delivery Reviews* **61**:4, 303-309. [CrossRef]
9. Pin-Lan Li , Erich Gulbins . 2007. Lipid Rafts and Redox Signaling. *Antioxidants & Redox Signaling* **9**:9, 1411-1416. [Abstract] [Full Text PDF] [Full Text PDF with Links]
10. Dipak K. Das Methods in Redox Signaling . [Citation] [Full Text HTML] [Full Text PDF] [Full Text PDF with Links]